New insigths on the metabolic diversity among the epibiotic microbial community of the hydrothermal shrimp Rimicaris exoculata

Magali Zbinden, Bruce Shillito, Nadine Le Bris, Constance De Villardi de Montlaur, Erwan Roussel, François Guyot, Françoise Gaill, Marie-Anne Cambon-Bonavita

New insigths on the metabolic diversity among the epibiotic microbial communitiy of the hydrothermal shrimp *Rimicaris exoculata.*

Magali Zbinden[a,ç], Bruce Shillito[a], Nadine Le Bris[b], Constance de Villardi de Montlaur[a], Erwan Roussel[c], François Guyot[d], Françoise Gaill[a], Marie-Anne Cambon-Bonavita[c]

[a] UMR CNRS 7138, Systématique, Adaptations et Evolution, UPMC, 7 Quai Saint Bernard, 75252 Paris cedex 05, France

[b] Département Environnement Profond, Ifremer DRO, BP 70, 29280 Plouzané, France

[c] Laboratory of Microbiology of Extreme Environments, Ifremer Brest, LM2E, UMR 6197, BP 70, 29280 Plouzané, France

[d] Institut de Physique du Globe de Paris, Laboratoire de Minéralogie-Cristallographie, Université Paris-Jussieu, Tour 16, Case 115, 4, place Jussieu, 75 252 Paris Cedex 05, France

Key words: high pressure experiments, hydrothermal vent shrimp, intracellular granules, iron, methane, sulfur

ç Corresponding author. Tel.: 00 33 1 44 27 35 02; Fax : 00 33 1 44 27 52 50.

***E-mail address*: magali.zbinden@snv.jussieu.fr**

Abstract.

The shrimp *Rimicaris exoculata* (Williams and Rona, 1986) dominates the megafauna of some of the Mid Atlantic ridge hydrothermal vent sites. This species harbors a rich community of bacterial epibionts inside its gill chamber. Literature data indicate that a single 16S rRNA phylotype dominates this epibiotic community, and is assumed to be a sulfide-oxidizing bacteria. However attempts of cultivation were not successful and did not allow to confirm it. The aim of our study was to test the hypothesis of sulfide oxidation in the gill chamber, by a multidisciplinary approach, using *in vivo* experiments at *in situ* pressure in the presence of sulfide, microscopic observations and a molecular survey. Morphology of microorganisms, before and after treatment, was analyzed to test the effect of sulfide depletion and re-exposure. Our observations, as well as molecular data indicate a wider diversity than previously described for this shrimp's epibiotic community. We observed occurrence of bacterial intracellular sulfur- and iron-enriched granules and some methanotrophic-like bacteria cells for the first time. Genes that are characteristic of methane-oxidizing (*pmoA*) and sulfide-oxidizing (APS*)* bacteria were identified. These results suggest that three metabolic types (iron, sulfide and methane oxidation) may co-occur within the epibiont community associated with *Rimicaris exoculata*. As this shrimp colonizes chemically contrasted environments, the relative abundance of each metabolic type could vary according to the local availability of reduced compounds.

1. Introduction

Hydrothermal vent communities along the Mid-Atlantic Ridge (MAR) are dominated by large populations of caridean shrimps. Found in dense clusters of 40 000 individuals per m^3 (Segonzac et al., 1993), *Rimicaris exoculata* is the most abundant species on some of these sites. This shrimp has been found to host a dense bacterial epibiosis on the internal walls (branchiostegites) of its branchial chamber and on its mouthparts (scaphognathites and exopodites of the first maxillipeds) (Van Dover et al., 1988; Casanova et al., 1993; Segonzac et al. 1993; Zbinden et al., 2004). This indicates an intimate association between these organisms. The main source of dietary carbon could originate: 1) from bacteria ingested with the sulfide scraped from the chimney (Van Dover et al., 1988), 2) from their epibiotic bacteria (Segonzac et al., 1993; Gebruk et al., 2000) or 3) from an autotrophic bacterial population living in the shrimp's gut (Pond et al., 1997; Polz et al., 1998; Zbinden and Cambon-Bonavita, 2003). Fatty acid abundances and carbon isotopic composition recently provided strong evidence that mature *R. exoculata* gain most of their carbon from the epibiotic bacteria within their carapace rather than from bacteria grazed on the chimney walls (Rieley et al., 1999). For shrimps sampled from the Snake Pit site, three bacterial morphotypes were described (Segonzac et al., 1993) which all belonged to the same phylotype of Epsilon*proteobacteria* (Polz and Cavanaugh, 1995). Although attempts to cultivate these microorganims failed until now, they were hypothesized to acquire their metabolic energy from sulfide oxidation (Gebruk et al. 1993; Wirsen et al., 1993). Chemosynthetic activity of the filamentous bacteria from the inner cephalothorax surface has been shown (Wirsen et al., 1993), but no significant increase of CO_2 incorporation was observed in the presence of reduced sulfur compounds (Polz et al., 1998).

More recently, Zbinden et al. (2004) suggested that another metabolic pathway, iron oxidation, could be involved at the iron-rich Rainbow ultramafic site. Unlike most active hydrothermal sites known to date, the hydrothermal circulation at Rainbow is hosted on mantle rocks. As a result, its fluid composition departs from the common range of hydrothermal end-members, and is relatively depleted in H_2S and enriched in H_2, FeII and CH_4, as a result of the serpentinization processes (Charlou et al., 2002; Douville et al., 2002). During the ATOS cruise shrimps were all collected from the Rainbow site. The main objective of our work was to test the hypothesis that all the shrimp epibionts were sulfide-oxidizers. To overcome the inhability to cultivate the epibionts, we performed *in vivo* experiments. For the first time, pressurized aquaria were used to gain information on the bacterial epibionts' metabolism. The aspect and ultrastructure of the bacteria were checked after incubations at 230 bars (*in situ* pressure), at 15°C (*in situ* temperature) with or without sulfide-enriched seawater (thereafter called sulfide pulses), and compared to *in situ* reference shrimps. A molecular survey was undertaken to get new insights on possible metabolic type of the epibiotic microbial communities of *Rimicaris exoculata*, particularly thiotrophy using the 5'-adenylylsulfate (APS) reductase gene.

2. Materials and methods

Animal collection and selection

Specimens of *Rimicaris exoculata* were collected during the French ATOS cruise (June 2001), on the Rainbow vent site (36°14.0' N, Mid-Atlantic Ridge, 2320 meter depth). Shrimps were collected with the suction sampler of the ROV "*Victor 6000*", operated from

the R/V "*L'Atalante*". Once on board, some live specimens were either immediately dissected into body components. These samples are referred to as "reference shrimps" further in the text. Alternatively, some shrimps were placed in pressure vessels (IPOCAMP™) for *in vivo* experiments (see below) and in this case dissected immediately after removal from the vessel. Scaphognathite samples were fixed in a 2.5% glutaraldehyde - sodium cacodylate buffered solution and later post-fixed in osmium tetroxide for morphological observations. Samples for X-ray analyses were not postfixed. For each treatment, shrimps in anecdysis were selected for observation according to the moult-staging method of Drach and Tchernigovtzeff (1967), by examination of bristle-bearing appendages (uropods) under a lightmicroscope. The moulting stage was later confirmed by examination of the branchiostegite integument by light microscopy and Transmission Electron Microscopy (TEM). For molecular studies, shrimps were frozen immediately after recovery under sterile conditions. Once in the lab, the scaphognathites and branchiostegites were dissected and DNA extraction was performed.

Pressurized incubator IPOCAMP™

The stainless steel pressure vessel has an internal volume of approximately 19 liters (see Shillito et al., 2001 for detailed description and diagrams). This is a flow-through pressure system, with flow rates that can reach 20 $l.h^{-1}$. Pressure oscillations arising from pump strokes (100 rpm) are less than 1 bar at working pressure. The temperature of the flowing seawater (filtered at 1 µm mesh) is constantly measured, at pressure, in the inlet and outlet lines (±1°C). Temperature regulation is powered by a regulation unit (Huber CC 240) that

circulates ethylene-glycol through steel jackets surrounding the pressure vessel and around the seawater inlet line.

***In vivo* experiments**. Re-pressurization at 230 bars was achieved in about 2 min after closure of the vessel. As the shrimps were sampled at the end of the dive, less than 2 h passed between the time the samples began decompression (submersible ascent) and the moment they were re-pressurized. At atmospheric pressure, just after the submersible recovery, the shrimps (except for some individuals, which may have been damaged by the suction sampler) were alive and active. Pressure vessel experiments were carried out at *in situ* pressure (230 bars) and at 15°C, according to the literature data: 10-15°C (Segonzac et al., 1993) ; 3.8-14.7°C (Zbinden et al., 2004) ; 13.2 ± 5.5°C (Desbruyères et al., 2001). Previous *in vivo* experiments showed a good physiological state of the shrimps when re-pressurized at these temperature and pressure conditions (Ravaux et al., 2003). Only alive and active shrimps after treatment were used for the present study.

Two experiments at 230 bars were performed:

(1) Sample incubation at 15°C in surface seawater, to investigate the effect of depletion of electron donors on the shrimps and their epibionts. Twelve shrimps were placed in the pressure vessel, for 30 h. The seawater was regularly (5 times) renewed, by replacing a quarter of the total volume. Surface seawater oxygen level (253 µM) lies slightly above the concentration measured in the environment of the shrimps (Schmidt et al., in press). These samples are referred to as "non-sulfide shrimps" further in the text.

125 (2) Incubation at 15°C, with exposure to sulfide pulses. Nine shrimps were placed in the
126 pressure vessel for 32 h. During the 32 h of the experiment, we first maintained the shrimps in
127 normal sea-water for 8 hours. Then, 4 pulses were performed as follows : i) the inlet of the
128 flow-through pressure system was fed with a reservoir containing 20 l of a solution of 25 µM
129 sulfide in natural surface seawater. This concentration roughly corresponds to the maximum
130 of estimated from the shrimps environment at Rainbow (Schmidt et al., in press). This
131 moderate concentration also ensured that the oxygen is not fully depleted from the medium.
132 When the reservoir was almost empty, the outlet line was connected to the inlet line, in order
133 to recirculate the sulfide-enriched seawater; ii) After an exposure of one hour, seawater was
134 then pumped into the vessel for 2h ; iii) finally the vessel was closed for 3h before the next
135 pulse started with a freshly prepared 25 µM sulfide solution. These samples are referred to as
136 "sulfide shrimps" further in the text. The term "re-pressurised shrimps" englobes both "non
137 sulfide" and "sulfide" shrimps.
138 Survival of the re-pressurized shrimps was determined at the end of the pressure experiments,
139 by identifying each individual and witnessing its movements.
140

141 **Light microscopy and transmission electron microscopy (TEM)**
142 Samples were dehydrated in ethanol and propylene oxide series and then embedded in an
143 epoxy resin (Serlabo). Semi-thin and ultra-thin sections were made on a Reichert-Jung
144 Ultramicrotome (Ultracut E) using a diamond knife. Semi-thin sections were stained with
145 toluidine blue for observations by light microscopy (using a Nikon Optiphot-pol microscope
146 and a Zeiss Opton photomicroscope). For ultrastructural observations, thin sections were laid

147 on copper grids and stained with uranyl acetate and lead citrate. Observations were carried out
148 on a Philips 201 TEM, operating at 80 kV.
149
150 **Energy dispersive X-ray microanalyses (EDX)**
151 Microanalysis was carried out using a JEOL JEM 2100F transmission electron microscope,
152 operating at 200 kV, and acquired with an energy dispersive X-ray detection system (Tracor
153 5400 FX), equipped with a Si(Li) diode, using a 2.4 nm probe.
154
155 **Ultrastructural analyses and enumeration of bacteria**
156 Exhaustive analysis and enumeration of bacteria and their intracellular granules were
157 undertaken on one individual for each treatment. For each shrimp, bacteria associated to 5
158 setae of the scaphognathite were analyzed. For each seta, an overall picture was taken and
159 picture of all the bacteria were then captured at a magnification of 20000. Bacteria cells were
160 then counted and described. The occurrence of intracellular granules was noted for each cell.
161 Granules were defined as electron-dense spots larger than 1.5 mm on the pictures (i.e. 75 nm),
162 as numerous dark spots of various sizes occur in the cells. Due to their small size, spots
163 smaller than 75 nm cannot be analyzed by EDX and were not taken into account in this study
164 because of the uncertainty on their nature.
165
166 **Statistical analyses**
167 A one-way ANOVA was used to test differences in the state of the bacteria (i.e. percentage of
168 full granules) among treatments. Normality was judged visually from normal probability plots

and homogeneity of variances was verified with the Levene test. A multiple range test using the Student-Newman-Keuls (SNK) procedure was performed to investigate the difference between treatments for significant results. All data analyses were carried out using Statistica v. 6 software.

DNA extraction

One *in situ* reference shrimp was dissected under sterile conditions. DNAs from scaphognathite (SC) and branchiostegite (LB), were extracted using the FastDNA SPIN kit for soil samples (Bio 101 System, Qbiogen) following the kit protocols.

PCR and cloning

PCR were performed using the universal primers for Bacteria or Archaea 16S rDNA on both (SC and LB) extracted DNA samples: E8F (AGA GTT TGA TCA TGG CTC AG) and U1492R (GTT ACC TTG TTA CGA CTT) for Bacteria and A8F (CGG TGG ATC CTG CCG GA) and A1492R (GGC TAC CTT GTT ACG ACT T) for Archaea. PCR cycles were as follows : 1 cycle of 3 min at 94°C, 30 cycles of 1 min at 94°C, 1 min 30 at 49°C and 2 min at 72°C and 1 cycle of 6 min at 72°C.

The gene encoding particulate methane monooxygenase subunit A (*pmoA*) was amplified on the SC DNA using the primers described by Duperron et al. (2007a) A189F (GGN GAC TGG GAC TTC TGG) and MB661R (CG GMG CAA CGT CYT TAC C). PCR cycles were as follows : 1 cycle of 4 min at 92°C , 30 cycles of 1 min at 92°C, 1 min 30 at 55°C and 1 min at 72°C and 1 cycle of 9 min at 72°C.

The gene encoding the APS reductase gene was amplified on the SC DNA using the primers designed before (Blazejak et al., 2006). PCR cycles were as follows : 1 cycle of 4 min at

92°C , 30 cycles of 1 min at 92°C, 1 min 30 at 58°C and 1 min at 72°C and 1 cycle of 9 min at 72°C.

Approximately 100 ng of bulk DNA was amplified in a 50 µl reaction mix containing (final concentration) : 1X Taq DNA polymerase buffer (Q biogen Starsbourg, France), 2 µM of each dNTP, 20 µM of each primer and 2.5U of Taq DNA polymerase (Q Biogen France). PCR products were then visualized on an agarose gel containing ethidium bromide before cloning. The PCR products were cloned with the TOPO TA Cloning kit (Invitrogen Corp., San Diego CA USA) following to the manufacturer's protocol. PCR products were purified using the QIAquick PCR purification kit (Qiagen SA, Grenoble, France) following the manufacturer's instructions. Clone libraries were constructed by transforming *E. coli* TOP10F'. Clones were selected on Petri dishes containing ampicilline (50µg/ml) and XGAL and IPTG for the white – blue selection. White clones were then cultured and treated for sequencing at the "Ouest Genopole Plateforme" (Roscoff, France, http//www.sb-roscoff.fr/SG/) on a Abi prism 3100 GA (Applied Biosystem), using the Big-Dye Terminator V3.1 (Applied Biosystem) following the manufacturer's instructions.

Phylogenetic analyses

To determine approximate phylogenetic affiliations, sequences were compared to those available in databases using the BLAST network service (Altschul et al., 1990). Alignments of 16S rDNA sequences were performed using CLUSTALW (Thompson et al., 1994), further refined manually using SEAVIEW (Galtier et al., 1996). The trees were constructed by PHYLO-WIN (Galtier et al., 1996). Only homologous positions were included in the phylogenetic comparisons. For the 16S rDNA phylogenetic reconstruction, the robustness of inferred topology was tested by bootstrap resampling (500) (Felsentein, 1985) of the tree

calculated on the basis of evolutionary distance (Neighbor-Joining-algorithm ; Saitou et al., 1987) with Kimura 2 correction. Sequences displaying more than 97% similarity were considered to be related, and grouped in the same phylotype. Phylogenies of amino acid sequences of the pmoA (154 aa) and APS (129 aa) were reconstructed using PHYLO-WIN with Neighbor-Joining-algorithm and PAM distance (according to Dayhoff's PAM model). The robustness of the inferred topology was tested by bootstrap resampling (500).

Nucleotide sequence accession numbers. Sequences have been deposited at EMBL with accession numbers: from **AM412507 to AM412521** and from **AM902724 to AM902731** for partial 16S rDNA sequences; from **AM412502 to AM412506** for partial *pmoA* (particulate methane monooxygenase subunit A) gene; and from **AM902732 to AM902736** for APS reductase gene.

3. Results

Morphology and ultrastructure of the epibionts

A total of 315 pictures was analyzed on which 6567 bacterial cells were counted. On *in situ* reference shrimps, TEM observations of the scaphognathite bacteria revealed more morphological diversity (figure 1) than previously described by Scanning Electron Microscopy (SEM) studies (Segonzac et al., 1993 ; Zbinden et al., 2004).

We observed 3 types of filaments (two thin types and one large) and two types of rods. Dimensions are in the range of those previously found (table 1). Two types of rods can be distinguished based on size, location and aspect of the intracellular contents. The first type

(figure 1b) is characterized by short and thick cells, with a dense dark intracellular content. They are mainly located on the setae. The second type (figure 1b) is longer and thinner, with a light intracellular content. These rods are mainly located on the barbula that emerge from the setae. Two types of thin filaments can be distinguished based on the aspect of the intracellular contents : i) a small number of thin filaments exhibit rectangular cells with no marked narrowing between two adjacent cells. Cells in these filaments show a homogeneous and dense content, with few electron light areas and no granules (figure 1d) ; ii) the others, more numerous, exhibit ovoid-shaped cells, with marked narrowing between two adjacent cells. Cells of these filaments have a more heterogeneous intracellular content (which seems denser at the periphery and more diffuse in the center) and contain granules (figure 1e).

Ultrastructural changes are observed between the bacteria of re-pressurised shrimps and those of reference shrimps (figure 2). No significant morphological differences were noticed between the bacteria of the shrimps from both pressure experiments. Cells of large and thin filaments, as well as thick rods, have a less regular shape and exhibit a more heterogeneous intracellular content than those of reference shrimps (figure 2b-c). Only thin rods keep the ultrastructal aspect observed in reference shrimps. Some of the bacteria show a globular intracellular content (figure 2d) or additional membrane folds (figure 2e). These types are only observed among bacteria of the shrimps maintained at 230 bars. Occasionally, these morphotypes can have a very degraded aspect, with totally mis-shapen cells (figure 3a), completely globular cell contents (figure 3c) or cell ghosts (figure 3c). Cell ghosts are also occasionally observed among bacteria of reference shrimps where they represent 1.5 to 4% of all the bacteria, and may be due to the usual turn-over of the cells. Cells with irregular shape and contents account for up to 30% of all cells in the re-pressurised shrimps and ghosts up to

15% (intra-individual variation between the five setae is too high to test the significance of inter-individual variations and the effect of sulfide exposure). Furthermore, very few dividing cells were observed for re-pressurised shrimps, whereas they were numerous for *in situ* reference shrimps. Surprisingly we observed, for the first time among *R. exoculata* epibionts (in reference shrimps, as well as in re-pressurised ones), some bacteria with stacks of intracytoplasmic membranes typical of methanotrophs (figure 2f) in both reference and re-pressurised shrimps.

Intracellular electron dense granules

Only granules larger than 75 nm in diameter were considered, the largest measuring up to 200 nm. Spots under 75 nm were counted separately, as "spots". The number of granules and spots is higher for reference shrimps than for re-pressurised ones (table 2). Granules occurred only in one type of thin filament, and are absent from thick filaments and rods. A given cell may contain several granules and spots (up to 7 granules and 10 spots per cell).

In the reference shrimps, most of the granules appear full (i.e they are electron dense and appear black on micrographs, figure 4a), whereas most appear partially or completely empty for the re-pressurised shrimps (i.e they are electron light and appear, at least partly white on micrographs, figure 4b). Percentage of full granules for each experiment are illustrated on figure 5. The percentage of full granules differs significantly between reference and re-pressurised shrimps (one-way ANOVA test; $F = 76.942$, $p < 10^{-6}$), although no significant difference was detected between sulfide and non-sulfide shrimps at 230 bars (SNK a posteriori test, $p > 0.05$).

284

285 **Chemical composition of granules**

286 An EDX microanalysis was performed in order to determine the elemental composition of the
287 granule content (figure 6). The control spectrum from the cytoplasmic area of the bacteria
288 showed copper (Cu) peaks due to the support grid, uranyl (U) peaks due to uranyl acetate
289 staining, and traces of chloride (Cl) due to the epoxy resin. Two types of granules were
290 analyzed. The first type contains 2 main peaks : phosphorus (P) and iron (Fe), in some cases
291 associated with small amounts of calcium (Ca) (not shown). The second type of granules
292 shows a single peak of sulfur (S). Occasionally, traces of iron (Fe) are detected (but it can be
293 due to the close occurrence of a thick iron oxide layer that surrounds some bacteria).

294

295 **Preliminary screening of bacterial diversity**

296 DNA was successfully extracted from scaphognathite and branchiostegite samples. PCR
297 amplifications for Archaea failed regardless of the conditions tested, even with nested PCR.
298 For Bacteria, 69 clones were sequenced for the scaphognathite and 56 for the branchiostegite
299 of an reference shrimp. Only 53 clones sequences were kept for the scaphognathite sample
300 and 46 for the branchiostegite sample, the other clone sequences being too short or of bad
301 quality. No chimera was detected in our study.
302 All the sequences are related to the *Proteobacteria* cluster (figure 7), mainly within the
303 Epsilon and Gamma groups, the Alpha and Delta*proteobacteria* being less abundant. One
304 group of 19 sequences is related to the *R. exoculata* gut clone 15, found in a previous study on
305 the gut of a specimen from the same vent site (Zbinden and Cambon-Bonavita, 2003). A

306 second group of 13 sequences is related to sequences retrieved from a vent gastropod coming
307 from Rodriguez Triple junction in the Indian Ocean (Goffredi, 2004). A third group (5 clone
308 sequences) is related to the *Rimicaris exoculata* epibiont (Polz and Cavanaugh, 1995).
309 Nineteen clones sequences are related to the *Rimicaris exoculata* gut clone 22 (Zbinden and
310 Cambon Bonavita, 2003). Six clone sequences are related to the Delta*proteobacteria*. Twenty
311 four sequences are affiliated to the Gamma*proteobacteria*. These latter are related to
312 sequences retrieved on a vent gastropod (Goffredi, 2004) and also to clone sequences
313 retrieved on carbonate chimney from the Lost City vent field (Brazelton et al., 2006). The last
314 group comprises eight clones, related to the Alpha*proteobacteria*, close to *Marinosulfomonas*
315 *methylotropha*, and to a clone isolated from Lost City vent field (Brazelton et al., 2006).
316

317 ***pmoA* and APS sequence analyses**

318 We successfully amplified the *pmoA* and APS reductase genes using DNA extracted from the
319 scaphognathite. Fifteen clones were sequenced for the *pmoA* and 5 for the APS reductase. All
320 the sequences were kept for the phylogenetic analyses. For the *pmoA* gene (Figure 8), two
321 clone sequences are affiliated to the *Methylobacter* sp. group, two clones sequences are
322 affiliated to a *Bathymodiolus* symbiont sequence and 11 clones sequences are affiliated to the
323 *Methylomonas methanica*. For the APS reductase gene (Figure 9), 5 sequences were related to
324 the Delta*proteobacteria.* Ninety sequences were only marginally related to the
325 Gamma*proteobacteria* APS gene (83% of similarity) and were related to the *Idas* thiotrophic
326 clone (Duperron et al. 2007b).

As no genes, until now, of the iron-oxidation pathway for neutrophilic iron-oxidizing bacteria are known, this metabolic pathway cannot be investigated by this method.

4. Discussion

Is sulfide oxidation active in the epibiotic community ?

Transmission electron microscopy allowed us to refine the morphological descriptions of the epibionts on the reference shrimps, detecting two types of thin filaments, and two types of rods, in addition to the thick filaments. These results indicate that the morphological diversity of bacteria associated with *R. exoculata* is higher than previously reported (Casanova et al., 1993; Gebruk et al., 1993 ; Zbinden et al., 2004). The molecular survey supports this result. Even though additionnal sequence investigations are needed to fully describe the microbial diversity within the gill chamber, the present study provides a preliminary overview of the epibiotic community composition. Many Epsilon*proteobacteria* sequences are related to microbial diversity usually associated with various hydrothermal invertebrates (*Alvinella pompejana*: Alain et al., 2002; *Paralvinella palmiformis*: Alain et al., 2004; gastropods: Goffredi et al., 2004; Suzuki et al., 2005; and *Rimicaris exoculata* gut: Zbinden and Cambon-Bonavita, 2003) and to the MAR environment (Lopez-Garcia et al., 2002). Only five sequences are slightly related to "*Rimicaris exoculata* ecto-epibiont". The Delta*proteobacteria* diversity is restricted to one cluster, and is related to an uncultured bacterium colonizing the mineral surfaces of a sulfide-microbial incubator. These microorganisms are usually thought to play a role in the sulfur cycle. In addition, we obtained APS reductase gene sequences that are related to those of the *Desulfobulbaceae* (Friedrich,

2002) known to be thiotroph. Most of the APS gene sequences obtained were related to the *Idas* thiotrophic symbiont gene (Duperron et al., 2007b), which is a Gamma*proteobacteria*, but with a low level of similarity (83%). In our phylogenetic survey, we did not obtain any 16S rDNA gene sequence related to thiotrophic Gamma*proteobacteria*, so it is unlikely that our APS gene sequences are related to these Gamma*proteobacteria*. As no Epsilon*proteobacteria* APS gene sequence is available in databanks, our APS gene sequences are more likely related to the numerous Epsilon*proteobacteria* identified in the phylogenetic survey. It is noteworthy that the APS gene can be transferred laterally among Bacteria. It is therefore not a good phylogenetic marker (Friedrich, 2002; Meyer and Kuever, 2007).

Bacteria associated with re-pressurised shrimps exhibit different ultrastructures compared to the reference shrimps. A mean of 30% of the epibionts display what we interpret as a degraded aspect (i.e. heterogeneous or globular cellular content, irregular wall shapes, cell ghosts). In addition, the number of dividing cells is higher for the reference shrimps, indicating a better physiological state. These results could indicate that some of the bacteria cannot withstand the chemical environment of the re-pressurisation experiments, whether or not sulfides are present.

TEM observations of the epibionts reveal the massive occurrence of intracellular granules. Such granules are often present in prokaryotic organisms (Shively, 1974). They comprise polyglucoside, polyphosphate granules, crystals or paracrystalline arrays such as magnetosomes (Fe_3O_4), poly-ß-hydroalkanoate (PHA) and sulfur globules. The main roles of these granules are hypothesized to be storage forms of energy and/or of various compounds

such as carbon, sulfur and phosphates. They can also play a part in detoxification processes. X-ray analyses indicate that there are two type of granules, one type containing phosphorus (P) and iron (Fe), most probably under polyphosphate form; the other type containing mainly sulfur (S). Several granules can occur in one bacterial cell, but they are always of the same type. The maintenance in a pressurized aquarium lead to the emptying of most of the granules, which suggests a storage role. Addition of sulfide does not affect this emptying phenomenon. However, the granules were counted as a whole, as it was no longer possible to morphologically distinguish the polyphosphate from the sulfur granules. It is conceivable that the slightly higher percentage of full granules, counted in the bacteria that received sulfide pulses (see figure 5), is due to a better conservation of the sulfur granules. *R. exoculata* epibionts (from the Snake Pit site) were hypothesized to acquire their metabolic energy from sulfide oxidation. At the ultrastructural level, sulfur-oxidizing bacteria are characterized by the accumulation of large granules of elemental sulfur, which is known to dissolve in solvents like those commonly used for classical TEM preparations (Vetter, 1985). Consequently, these globules appear empty in thin sections (Lechaire et al., 2006). On our sections, the granule contents were not removed during preparation steps, which suggests that they are not elemental sulfur under the form usually found in sulfur-oxidizing bacteria. We can then hypothesize that these granules are rather formed of another type of more stable cristalline sulfur or are sulfur-rich organic matter. Nevertheless, sulfur-containing biopolymers are rare : they are mostly proteins containing methionine and cysteine, or complex polysaccharides that contain sulfate groups. PTE (polythioester), a new class of sulfur-containing polymer, have recently been described, (Lütke-Eversloh et al., 2001). It belongs to the polyhydroxyalkanoates (PHAs), a class of biopolymers known to occur abundantly as storage

394 compounds for energy and carbon, in a large variety of bacteria and archaea (Anderson and
395 Dawes, 1990).
396 Taken all together, the TEM observations of bacteria associated to re-pressurised shrimps
397 show a low positive impact of sulfide reexposure. Three hypotheses could thus be put
398 forward to explain this: 1) the concentration and frequency of the pulses were insufficient to
399 allow a good maintenance of the epibionts, or 2) these bacteria do not all rely on sulfide for
400 their growth, or 3) the chemical composition of the fluid in the pressure vessel was not
401 adapted for epibiont growth that may require more complex substrates as suggested by the
402 lack of cultures despite many attempts. Considering the results of previous work on the
403 epibionts of *R. exoculata* (Zbinden et al., 2004) and the chemistry of this peculiar
404 environment : low sulfide but high iron and methane concentration (Charlou et al., 2002 ;
405 Douville et al., 2002), it is possible that some bacteria do not rely on sulfide oxidation but
406 rather on iron or methane oxidation.
407
408 **Occurrence of iron oxidation among the epibiotic community**
409 Genes involved in iron oxidation at neutral pH are still unknown and iron oxidizers show a
410 broad diversity among the *Proteobacteria* (Edwards et al., 2003). So, iron oxidation
411 metabolism could not be studied through a molecular approaches. Nevertheless, iron
412 polyphosphate granules were detected inside the epibiont cells. Polyphosphate granules are
413 widely distributed in prokaryotes, ranging in diameter from 48 nm to 1µm (Shively, 1974).
414 Putative roles of polyphosphate are numerous : ATP substitute, energy storage or chelator of
415 metal ions (Kornberg, 1995). Lechaire et al. (2002) described the occurrence of iron
416 polyphosphates granules in bacteria associated with the tube of *Riftia pachyptila*, a

417 hydrothermal vent vestimentiferan. Since polyphosphates are known to fluctuate in response
418 to nutritional and other parameters, these authors suggest that they could act as a reservoir of
419 oxygen in the case of environmental anoxia. As the occurrence of iron-oxidizers among the
420 bacteria has been suggested (Zbinden et al., 2004), these granules could be a reservoir for
421 iron. Alternatively, if these granules occur in non-iron oxidizing bacteria, the chelation of iron
422 by the polyphosphate granules could reduce its toxicity for the cell.
423 Anyway, the only way to certify the occurrence of iron-oxidizing bacteria among the
424 epibionts is to successfully cultivate and isolate these strains. Such attempts are under
425 progress in our lab.
426

427 **A possible alternative metabolism : methanotrophy and methylotrophy**

428 A sixth morphotype, bacteria with stacks of intracytoplasmic membranes typical of type I
429 methanotrophs, was observed for the first time among *R. exoculata* epibionts. Moreover, our
430 sequences cluster with known Gamma*proteobacteria* methanotrophic epibionts sequences,
431 such as *Bathymodiolus* methanotrophic gill symbionts (Duperron et al., 2005). This is also
432 supported by our three groups of *pmoA* sequences that clearly belong to the methylotrophic
433 Gamma*proteobacteria* class (*Methylomonas* sp., *Methylobacter* sp. and *Bathymodiolus pmoA*
434 gene sequences). In addition, some clone sequences are related to Alpha*proteobacteria*
435 methylotroph species and to Epsilon*proteobacteria* clone sequences retrieved from enriched-
436 methane environments such as the MAR Lost City and Rainbow sites, or to the Milano mud
437 volcano (Figure 7).
438

Co-occurrence of different metabolic types in the epibiotic community

Taken all together, our microscopic observations and molecular data seem to indicate that at least three metabolic types could co-occur among the epibiotic microbial community associated to *R. exoculata* at Rainbow: iron-oxidation, methanotrophy and thiotrophy. Desbruyères et al. (2001) tried to correlate biological diversity to the varying composition of end-member fluids. According to the amount of iron oxide closely associated to the epibionts (Zbinden et al., 2004), and to the high level of ferrous iron in the pure fluids (Charlou et al., 2002), we suggest that iron oxidation may be the dominant metabolism for this site. Recently, Salerno et al. (2005) correlated the relative microbial abundance of epibiont types of two species of mussels (*Bathymodiolus azoricus* and *B. heckerae*) with the availability of CH_4 and dissolved H_2S in the end-member fluids. They found that when the CH_4:H_2S ratio was less than 1 (as for Snake Pit, Campbell et al., 1988) then thiotrophic epibionts were dominant. If the ratio was greater than 2 (as for Lost City, Kelley et al., 2001) then methanotrophs were the dominant epibionts. For Rainbow, the ratio of CH_4:H_2S varies from 1.54 to 2.61 in pure fluids (Charlou et al., 2002). Applying the Salerno et al. (2005) empirical model to *Rimicaris* epibionts at Rainbow, would suggest that methanotrophy is an important metabolic pathway, possibly dominating sulfide oxidation. Sampling and *in situ* measurements in shrimp swarms provide nevertheless a more realistic picture of the environmental conditions experienced by the shrimps. A recent study on potential electron donors for microbial primary production within the swarms at Rainbow indicates that ferrous iron is the most favorable energy source to support epibiotic growth. Methane and sulfide would appear as secondary energy sources in this environment, where hydrogen could also represent an altenative energy source for the epibionts (Schmidt et al., in press).

Conclusion

Based on TEM observations, and a preliminary molecular survey, the diversity of the *Rimicaris exoculata* epibionts (in terms of morphology and metabolism) appears to be higher than previously reported. Based on these results, we propose that the three metabolic types (iron, sulfur and methane oxidation) co-occur within the epibiont biomass associated with *Rimicaris exoculata*, and that the relative contribution of each metabolism may differ according to the local fluid chemical composition. A much wider scale study, with animals collected from chemically contrasted environments, is needed to better understand the connections of the epibiotic bacterial communities in response to the chemistry of the environment.

Acknowledgements. The authors wish to thank P.M. Sarradin, chief scientist of the ATOS cruise, as well as the captain and crew of the R/V Atalante and the Victor ROV team. The authors also thank Eric Thiébaut for his help with the statistical analyses, and Philippe Compère for his help in determination of the moulting stages. The author are also grateful to Stephane Hourdez for his review of the manuscript. Electron microscopy was performed at the Service de Microscopie Electronique, IFR 83 de Biologie Integrative-CNRS/Paris VI. This work was partly funded with the help of the MOMARNET and VENTOX (EVK3 CT-1999-0003) programs, Ifremer research institute and Région Bretagne and Ouest Génopole.

References

Alain, K., Olagnon, M., Desbruyères, D., Page, A., Barbier, G., Juniper, K., Quérellou, J., Cambon-Bonavita, M., 2002. Phylogenetic characterization of the bacterial assemblage associated with the hydrothermal vent polychaete *Paralvinella palmiformis*. FEMS Microbiol. Ecol. 42, 463-476.

Alain, K., Zbinden, M., Le Bris, N., Lesongeur, F., Querellou, J., Gaill, F., Cambon-Bonavita, M.-A., 2004. Early steps of colonisation processes at deep-sea hydrothermal vents. Environ. Microbiol. 6 (3), 227-241.

Altschul, S., Gish, W., Miller, W., Myers, E., Lipman, D., 1990. Basic local alignment search tool. J. Mol. Biol. 215, 403-410.

Anderson, A., Dawes, E., 1990. Occurence, metabolism, metabolic role, and industrial uses of bacterial polyhydroxyalkanoates. Microbiol. Rev. 54(4), 450-472.

Blazejak, A., Erseus, C., Amann, R., Dubilier, N., 2005. Coexistence of bacterial sulfide oxidizers, sulfate reducers, and spirochetes in a gutless worm (Oligochaeta) from the Peru margin. Appl. Environ. Microbiol. 71, 1553–1561.

Brazelton, W., Schrenk, M., Kelley, D., Baross, J., 2006. Methane- and sulfur-metabolizing microbial communities dominate the Lost City hydrothermal field ecosystem. Appl. Environ. Microbiol. 72 (9), 6257-6270.

Campbell, A., Palmer, M., Klinkhammer, G., Bowers, T., Edmond, J., Lawrence, J., Casey, J., Thompson, G., Humphris, S., Rona, P., Karson, J., 1988. The chemistry of springs on the Mid-Atlantic Ridge. Nature 335, 514-519.

Casanova, B., Brunet, M., Segonzac, M., 1993. L'impact d'une épibiose bactérienne sur la morphologie fonctionnelle de crevettes associées à l'hydrothermalisme médio-Atlantique. Cah. Biol. Mar. 34, 573-588.

506 Charlou, J. L., Donval, J. P., Fouquet, Y., Jean-Baptiste, P., Holm, N., Caccavo, F., 2002.
507 Geochemistry of high H_2 and CH_4 vent fluids issuing from ultramafic rocks at the Rainbow
508 hydrothermal field (36°14'N, MAR). Chem. Geol. 191, 345-359.
509 Desbruyères, D., Biscoito, M., Caprais, J. C., Colaço, A., Comtet, T., Crassous, P., Fouquet,
510 Y., Khripounoff, A., Le Bris, N., Olu, K., Riso, R., Sarradin, P. M., Segonzac, M.,
511 Vangriesheim, A., 2001. Variations in deep-sea hydrothermal vent communities on the Mid-
512 Atlantic Ridge near the Azores plateau. Deep-sea Res. PtI 48, 1325-1346.
513 Douville, E., Charlou, J. L., Oelkers, E. H., Bienvenu, P., Jove Colon, C. F., Donval, J. P.,
514 Fouquet, Y., Prieur, D., Appriou, P., 2002. The rainbow vent fluids (36°14'N, MAR): the
515 influence of ultramafic rocks and phase separation on trace metal content in Mid-Atlantic
516 Ridge hydrothermal fluids. Chem. Geol. 184, 37-48.
517 Drach, P., Tchernigovtzeff, C., 1967. Sur la méthode de détermination des stages d'intermue
518 et son application générale aux Crustacés. Vie Milieu 18A, 595-609.
519 Duperron, S., Nadalig, T., Caprais, J., Sibuet, M., Fiala-Médioni, A., Amann, R., Dubilier, N.,
520 2005. Dual symbiosis in a *Bathymodiolus* sp. mussel from a methane seep on the Gabon
521 continental margin (Southeast Atlantic): 16S rRNA phylogeny and distribution of the
522 symbionts in gills. Appl. Environ. Microbiol. 71(4), 1694-1700.
523 Duperron, S., Fiala-Médioni, A., Caprais, J. C., Olu, K., Sibuet, M., 2007a. Evidence for
524 chemoautotrophic symbiosis in a Mediterranean cold seep clam (Bivalvia: Lucinidae):
525 comparative sequence analysis of bacterial 16S rRNA, APS reductase and RubisCO genes.
526 FEMS Microbiol. Ecol. 59(1), 64-70.
527 Duperron, S., Halary, S., Lorion, J., Sibuet, M., Gaill, F., 2007b. Unexpected co-occurrence
528 of six bacterial symbionts in the gills of the cold seep mussel *Idas* sp. (Bivalvia: Mytilidae).
529 Environ. Microbiol. In press, doi:10.1111/j.1462-2920.2007.01465.x.

530 Edwards, K., Rogers, D., Wirsen, C., McCollom, T., 2003. Isolation and characterization of
531 novel psychrophilic, neutrophilic, Fe-oxidizing, chemolithoautotrophic a- and g-
532 Proteobacteria from the deep-sea. Appl. Environ. Microbiol. 69 (5), 2906-2913.
533 Felsentein, J., 1985. Confidence limits on phylogenies: an approach using the bootstrap.
534 Evolution 30, 783-791.
535 Friedrich, M., 2002. Phylogenetic analysis reveals multiple lateral transfers of adenosine-5'-
536 phosphosulfate reductase genes among sulfate-reducing microorganisms. J. Bacteriol. 1 (1),
537 278-289.
538 Galtier, N., Gouy, M., Gautier, C., 1996. SEAVIEW and PHYLO_WIN: two graphic tools for
539 sequence alignment and molecular phylogeny. Comput. Appl. Biosci. 12, 543-548.
540 Gebruk, A., Pimenov, N., Savvichev, A., 1993. Feeding specialization of bresiliid shrimps in
541 the TAG site hydrothermal community. Mar. Ecol. Prog. Ser. 98, 247-253.
542 Goffredi, S., Waren, A., Orphan, V., Van Dover, C., Vriejenhoek, R., 2004. Novel forms of
543 structural integration between microbes and a hydrothermal vent gastropod from the Indian
544 Ocean. Appl. Environ. Microbiol. 70 (5), 3082-3090.
545 Kelley, D., Karson, J., Blackman, D., Früh-Green, G., Butterfield, D., Lilley, M., Olson, E.,
546 Schrenk, M., Roe, K., Lebon, G., Rivizzigno, P., Party, t. A.-S., 2001. An off-axis
547 hydrothermal vent field near the Mid-Atlantic Ridge at 30°N. Nature 412, 145-149.
548 Kornberg, A., 1995. Inorganic polyphosphate : toward making a forgotten polymer
549 unforgettable. J. Bacteriol. 177 (3), 491-496.
550 Lechaire, J. P., Shillito, B., Frébourg, G., Gaill, F., 2002. Elemental characterization of
551 microorganism granules by EFTEM in the tube wall of a deep-sea vent invertebrate. Biol.
552 Cell 94, 243-249.
553 Lechaire, J., Frébourg, G., Gaill, F., Gros, O., 2006. In situ localization of sulphur in the

554 thiotrophic symbiotic model Lucina pectinata (Gmelin, 1791) by cryo-EFTEM microanalysis.
555 Biol. Cell 98, 163-170.
556 Lopez-Garcia, P., Gaill, F., Moreira, D., 2002. Wide bacterial diversity associated with tubes
557 of the vent worm *Riftia pachyptila*. Environ. Microbiol. 4(4), 204-215.
558 Lütke-Eversloh, T., Bergander, K., Luftman, H., Steinbüchel, A., 2001. Identification of a
559 new class of biopolymer : bacterial synthesis of a sulfur-containing polymer with thioester
560 linkages. Microbiology 147, 11-19.
561 Meyer, B., Kuever, J., 2007. Molecular analysis of the diversity of sulfate-reducing and
562 sulfur-oxidizing prokaryotes in the environment using aprA as functional marker gene. Appl.
563 Environ. Microbiol. Published online ahead of print on 5 October 2007. Doi: 10.1128 /
564 AEM.01272-07
565 Polz, M., Cavanaugh, C., 1995. Dominance of one bacterial phylotype at a Mid-Atlantic
566 Ridge hydrothermal vent site. Proc. Natl. Acad. Sci. USA 92, 7232-7236.
567 Polz, M., Robinson, J., Cavanaugh, C., Van Dover, C., 1998. Trophic ecology of massive
568 shrimp aggregations at a mid-Atlantic Ridge hydrothermal vent site. Limnol. Oceanogr.
569 43(7), 1631-1638.
570 Pond, D., Dixon, D., Bell, M., Fallick, A., Sargent, J., 1997. Occurence of 16:2(n-4) and 18:2
571 (n-4) fatty acids in the lipids of the hydrothermal vent shrimps *Rimicaris exoculata* and
572 *Alvinocaris markensis*: nutritional and trophic implications. Mar. Ecol. Prog. Ser. 156, 167-
573 174.
574 Ravaux, J., Gaill, F., Le Bris, N., Sarradin, P. M., Jollivet, D., Shillito, B., 2003. Heat-shock
575 response and temperature resistance in the deep-sea vent shrimp *Rimicaris exoculata*. J. Exp.
576 Biol. 206, 2345-2354.
577 Rieley, G., Van Dover, C., Hedrick, D., Eglinton, G., 1999. Trophic ecology of *Rimicaris*

578 *exoculata*: a combined lipid abundance/stable isotope approach. Mar. Biol. 133, 495-499.
579 Saitou, M., Nei, M., 1987. The neighbor-joining method : a new method for reconstructing
580 phylogenetic trees. Mol. Biol. Evol. 4, 406-425.
581 Salerno, L., Macko, S., Hallam, S., Bright, M., Won, Y., McKiness, Z., Van Dover, C., 2005.
582 Characterization of symbiont populations in life history stages of mussels from
583 chemosynthetic environments. Biol. Bull. 208, 145-155.
584 Schmidt, C., Vuillemin, R., Le Gall, C., Gaill, F., Le Bris, N., in press. Geochemical energy
585 sources for microbial primary production in the environment of hydrothermal vent shrimps.
586 Mar. Chem.
587 Segonzac, M., de Saint-Laurent, M., Casanova, B., 1993. L'énigme du comportement
588 trophique des crevettes Alvinocarididae des sites hydrothermaux de la dorsale médio-
589 atlantique. Cah. Biol. Mar. 34, 535-571.
590 Shillito, B., Jollivet, D., Sarradin, P. M., Rodier, P., Lallier, F., Desbruyères, D., Gaill, F.,
591 2001. Temperature resistance of *Hesiolyra bergi*, a polychaetous annelid living on vent
592 smoker walls. Mar. Ecol. Prog. Ser. 216, 141-149.
593 Shively, J., 1974. Inclusion bodies in prokaryotes. Annu. Rev. Microbiol. 28, 167–187.
594 Suzuki, Y., Sasaki, T., Suzuki, M., Nogi, Y., Miwa, T., Takai, K., Nealson, K., Horikoshi, K.,
595 2005. Novel chemoautotrophic endosymbiosis between a member of the epsilon-
596 proteobacteria and the hydrothermal-vent gastropod *Alviniconcha aff. hessleri* (Gastropoda:
597 Provannidae) from the Indian Ocean. Appl. Environ. Microbiol. 71(9), 5440-5450.
598 Thompson, J., Higgins, D., Gibson, T., 1994. CLUSTAL W : improving the sensitivity of
599 progressive multiple sequence alignment through sequence weighting, position-specific gap
600 penalties and weight matrix choice. Nucleic Acids Res. 22, 4673-4680.
601 Van Dover, C., Fry, B., Grassle, J., Humphris, S., Rona, P., 1988. Feeding biology of the
602 shrimp *Rimicaris exoculata* at hydrothermal vents on the Mid-Atlantic Ridge. Mar. Biol. 98,

603 209-216.

604 Vetter, R., 1985. Elemental sulfur in the gills of three species of clams containing
605 chemoautotrophic symbiotic bacteria: a possible inorganic energy storage compound. Mar.
606 Biol. 88, 33-42.

607 Williams, A., Rona, P., 1986. Two new caridean shrimps (Bresiliidae) from a hydrothermal
608 field on the Mid-Atlantic Ridge. J. Crustacean Biol. 6(3), 446-462.

609 Wirsen, C., Jannasch, H. W., Molyneaux, S., 1993. Chemosynthetic microbial activity at Mid-
610 Atlantic Ridge hydrothermal vent sites. J. Geophys. Res. 98 (B6), 9693-9703.

611 Zbinden, M., Cambon-Bonavita, M.-A., 2003. Occurence of *Deferribacterales* and
612 *Entomoplasmatales* in the deep-sea shrimp *Rimicaris exoculata* gut. FEMS Microbiol. Ecol.
613 46, 23-30.

614 Zbinden, M., Le Bris, N., Gaill, F., Compère, P., 2004. Distribution of bacteria and associated
615 minerals in the gill chamber of the vent shrimp *Rimicaris exoculata* and related
616 biogeochemical processes. Mar. Ecol. Prog. Ser. 284, 237-251.

617 **Figure legends**

618

619 **Figure 1:** Bacteria associated with a scaphognathite seta of a reference shrimp. **a)** General
620 view of the seta (s) and the associated bacteria. **b to e)** Observed morphotypes: **b)** rods type
621 (1) attached to the seta (s) and rods type (2) attached to the barbula (ba) ; **c)** large filaments; **e)**
622 thin filaments without granules inside the cells ; **d)** thin filaments with granules. Scale bars: a
623 = 5µm, b, c, d, e = 1 µm.

624

625 **Figure 2:** Bacteria associated with a scaphognathite seta of the re-pressurised shrimps. **a)**
626 General view of the seta and the associated bacteria. **b to e)** Observed ultrastructural
627 modifications: **b)** type 1 rods (type 2 does not seem to be affected); **c)** large filaments with
628 heterogeneous content; **d)** or with globular content; **e)** thin filaments with heterogeneous
629 content **(d)**, and occasionally occurrence of membrane folds at the boundary of the cell
630 (arrows). **(f)** methanotrophic bacteria characterized by their stacks of intracytoplasmic
631 membranes. Scale bars: a = 5µm ; b = 0.5 µm ; c, d, e, f = 1µm.

632

633 **Figure 3:** Evolution of the morphotypes observed in the re-pressurised shrimps. Filament
634 cells exhibit a mis shapen aspect (a), a completely globular content (b) or appear as ghosts (c).
635 Scale bars: a = 1µm ; b, c = 0.5µm.

636

637 **Figure 4:** Bacterial intracellular granules. Granules are full (arrows) in bacteria associated
638 with the reference shrimp **(a)** and mostly empty (arrows) in those associated with re-
639 pressurised shrimps **(b)**. Scale bars: a, b = 0.5µm.
640
641 **Figure 5:** Percentage of full granules in bacteria according to treatment. Diagram showing the
642 percentage of full granules per seta for *in situ* reference shrimp, and re-pressurised shrimps
643 either in seawater or submitted to sulfide pulses. The mean percentage for each treatment is
644 also given.
645
646 **Figure 6**: Elemental X-ray microanalyzes of the bacterial intracellular granules. Spectra were
647 obtained on a) the cytoplasm of the bacteria (as control), b) the first type of granule showing
648 major Fe and P peaks and traces of Si, c) the second type of granule, showing one major S
649 peak.
650
651 **Figure 7**: Phylogenetic trees obtained using Neighbor-Joining analysis with bootstrap
652 resampling (500 replicates). Topologies were confirmed with Maximum Parsimony method.
653 Bootstrap values are indicated on nodes above 70%. Accession numbers of the sequences
654 used are indicated on the tree (from AM412507 to AM412521 and from AM902724 to
655 AM902731).
656
657 **Figure 8:** Neighbor-Joining tree of pmoA amino acid sequences from *Rimicaris exoculata*
658 gill chamber epibionts based on 154 amino acid positions using PAM distance (according to

659 Dayhoff's PAM model). The robustness of the inferred topology was tested by bootstrap
660 resampling (500). Accession numbers of the sequences used are indicated on the tree (from
661 AM412502 to number AM412506).
662
663 **Figure 9:** Neighbor-Joining tree of APS reductase amino acid sequences from *Rimicaris*
664 *exoculata* gill chamber epibionts based on 129 amino acid positions using PAM distance
665 (according to Dayhoff's PAM model). The robustness of the inferred topology was tested by
666 bootstrap resampling (500). Accession numbers of the sequences used are indicated on the
667 tree (from AM902732 to AM902736).
668

Figure 1

Click here to download high resolution image

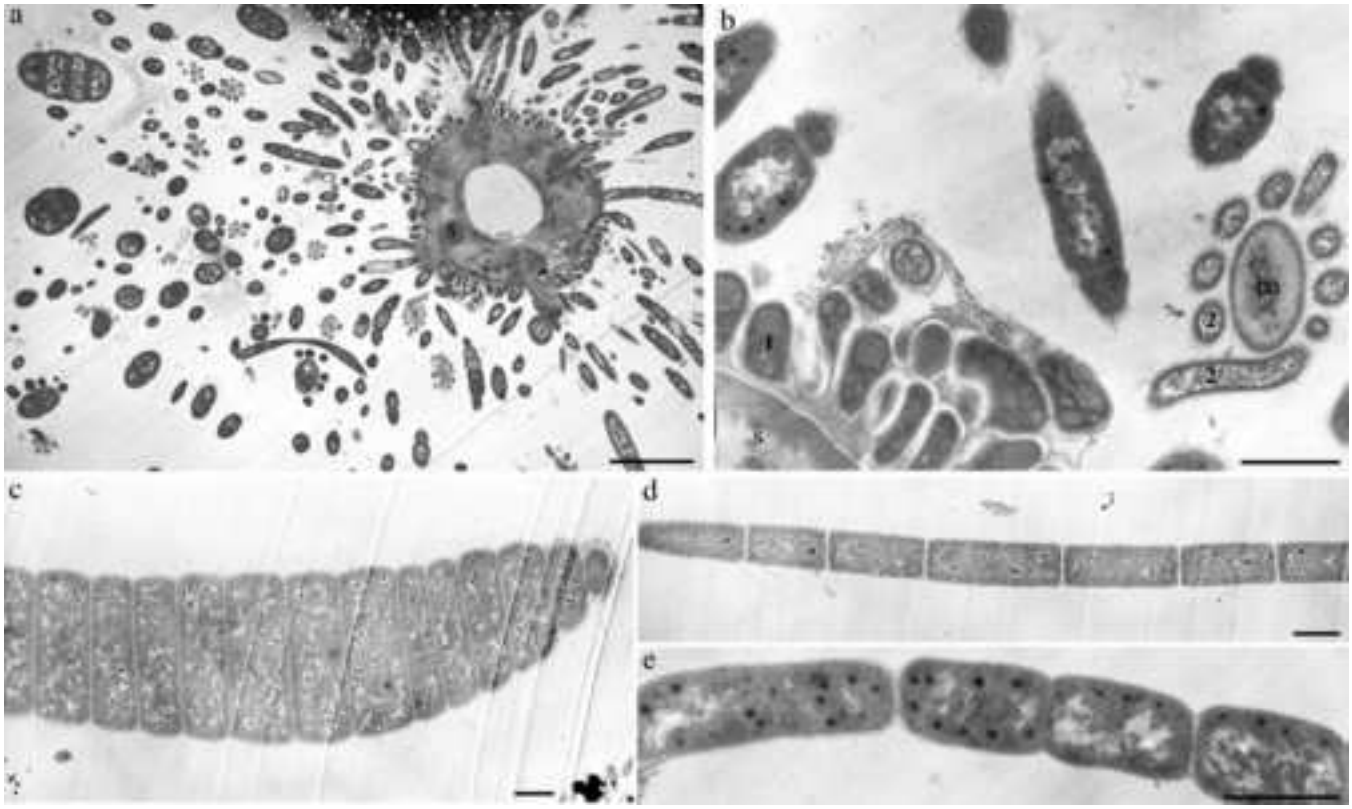

Figure 2

Click here to download high resolution image

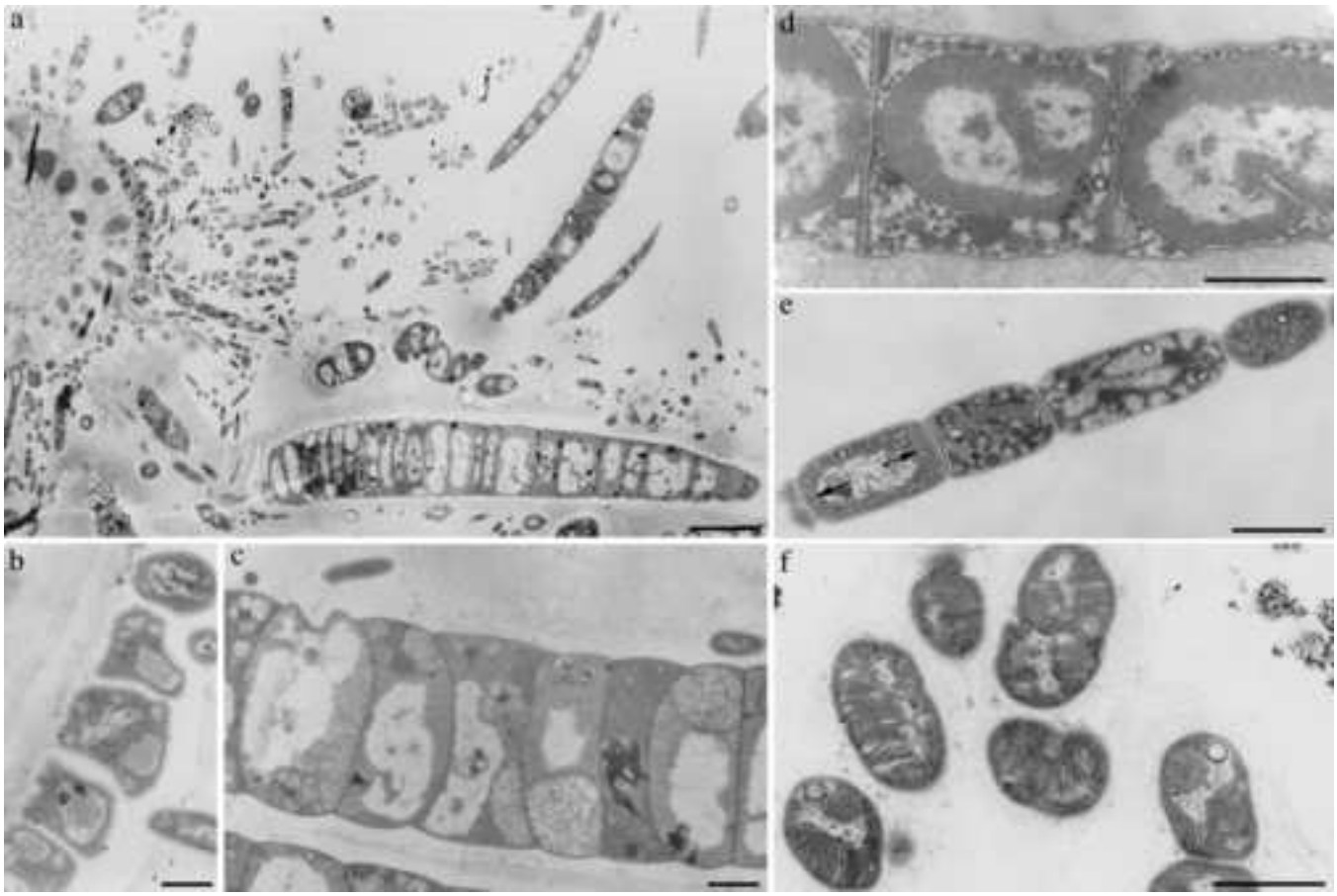

Figure 3

Click here to download high resolution image

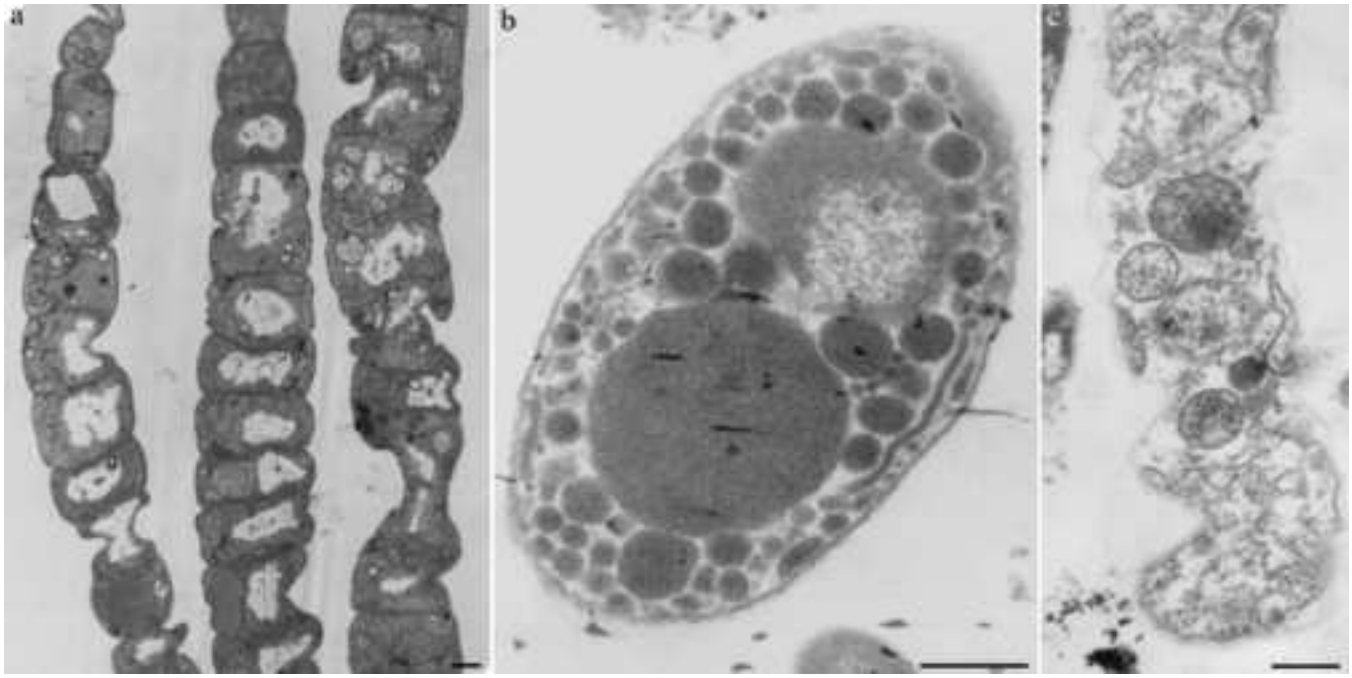

Figure 4

Click here to download high resolution image

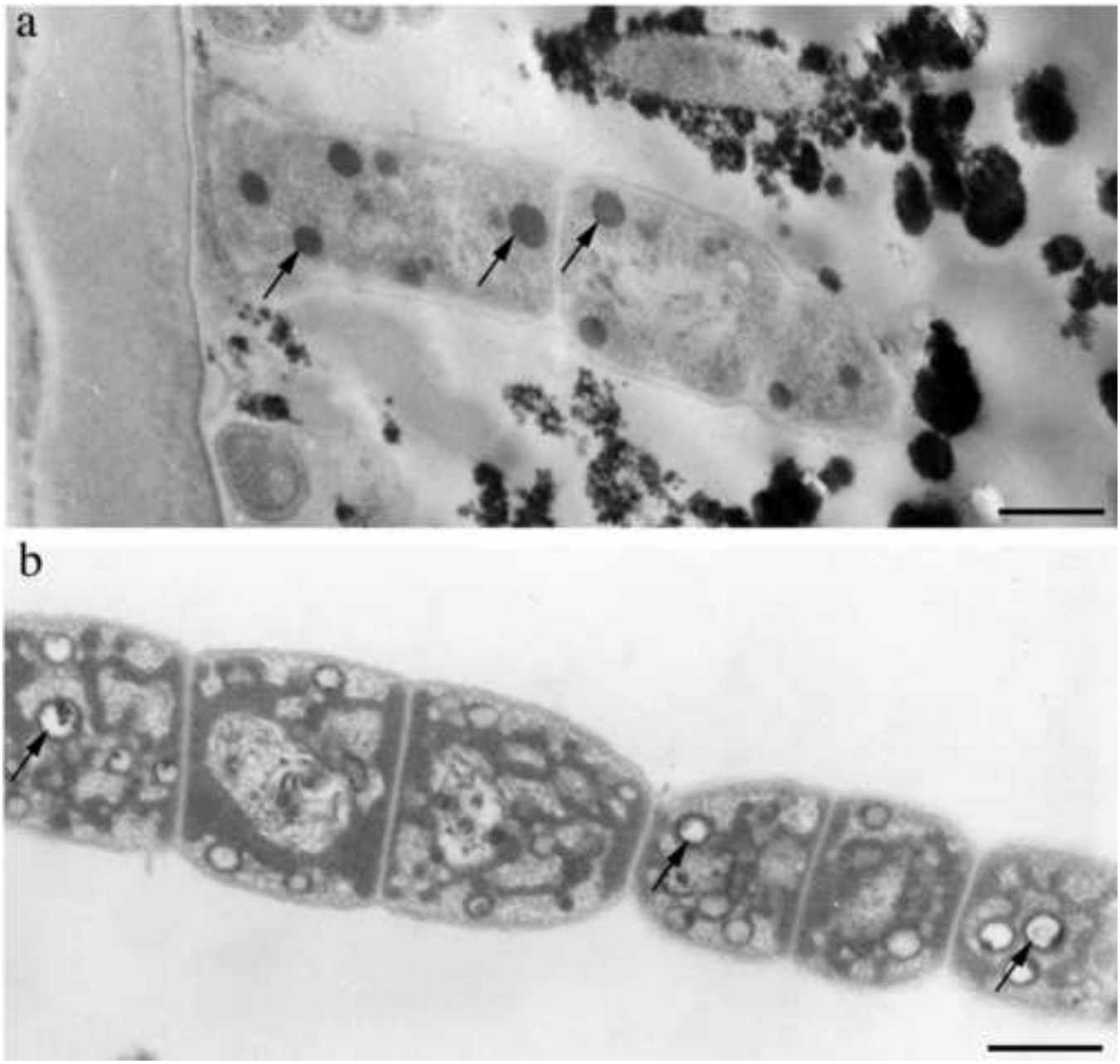

Figure 5

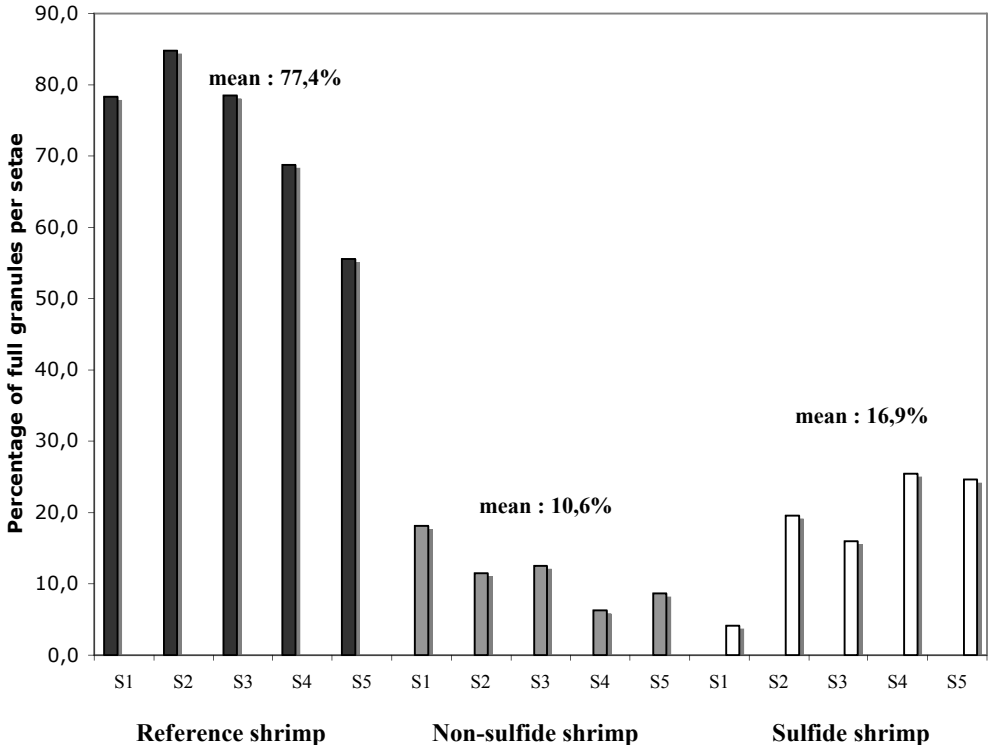
90,0
80,0
70,0
60,0
50,0
40,0
30,0
20,0
10,0
0,0
Percentage of full granules per setae
mean : 77,4%
mean : 10,6%
mean : 16,9%
S1
S2
S3
S4
S5
Reference shrimp
Non-sulfide shrimp
Sulfide shrimp

Figure 6

Click here to download high resolution image

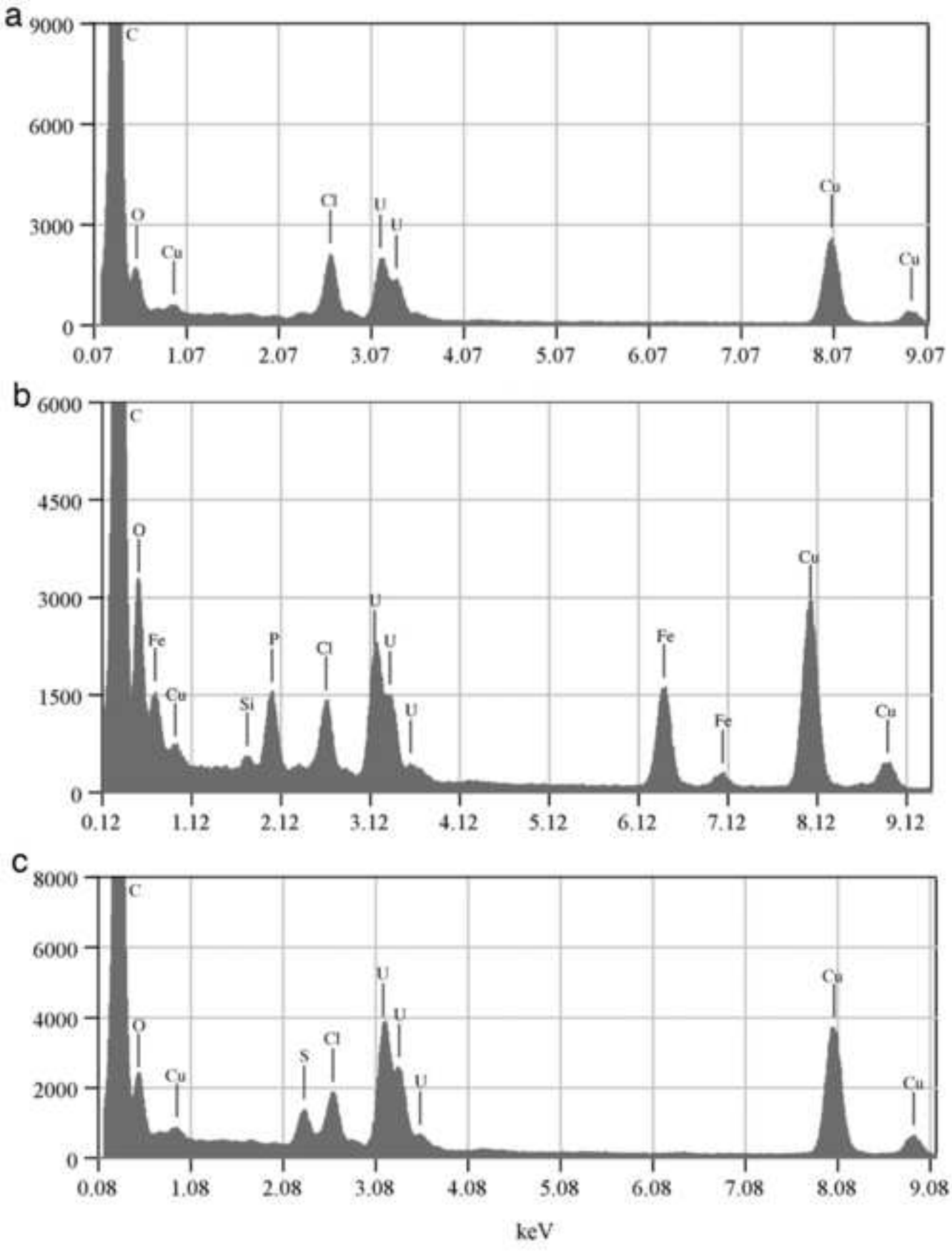

Figure 7

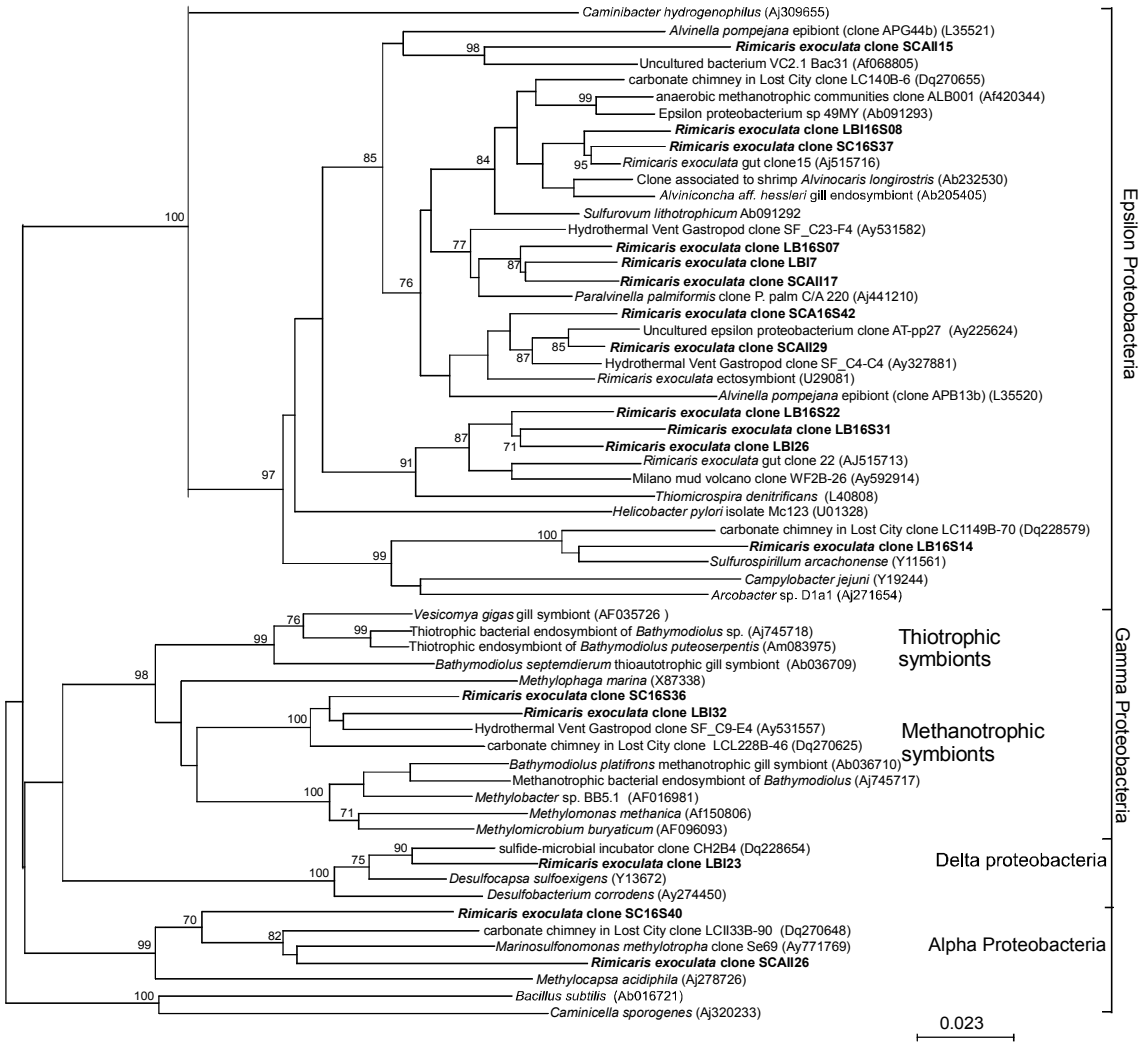
Caminibacter hydrogenophilus (Aj309655)
Alvinella pompejana epibiont (clone APG44b) (L35521)
Rimicaris exoculata clone SCAII15
Uncultured bacterium VC2.1 Bac31 (Af068805)
carbonate chimney in Lost City clone LC140B-6 (Dq270655)
anaerobic methanotrophic communities clone ALB001 (Af420344)
Epsilon proteobacterium sp 49MY (Ab091293)
Rimicaris exoculata clone LBI16S08
Rimicaris exoculata clone SC16S37
Rimicaris exoculata gut clone15 (Aj515716)
Clone associated to shrimp Alvinocaris longirostris (Ab232530)
Alviniconcha aff. hessleri gill endosymbiont (Ab205405)
Sulfurovum lithotrophicum Ab091292
Hydrothermal Vent Gastropod clone SF_C23-F4 (Ay531582)
Rimicaris exoculata clone LB16S07
Rimicaris exoculata clone LBI7
Rimicaris exoculata clone SCAII17
Paralvinella palmiformis clone P. palm C/A 220 (Aj441210)
Rimicaris exoculata clone SCA16S42
Uncultured epsilon proteobacterium clone AT-pp27 (Ay225624)
Rimicaris exoculata clone SCAII29
Hydrothermal Vent Gastropod clone SF_C4-C4 (Ay327881)
Rimicaris exoculata ectosymbiont (U29081)
Alvinella pompejana epibiont (clone APB13b) (L35520)
Rimicaris exoculata clone LB16S22
Rimicaris exoculata clone LB16S31
Rimicaris exoculata clone LBI26
Rimicaris exoculata gut clone 22 (AJ515713)
Milano mud volcano clone WF2B-26 (Ay592914)
Thiomicrospira denitrificans (L40808)
Helicobacter pylori isolate Mc123 (U01328)
carbonate chimney in Lost City clone LC1149B-70 (Dq228579)
Rimicaris exoculata clone LB16S14
Sulfurospirillum arcachonense (Y11561)
Campylobacter jejuni (Y19244)
Arcobacter sp. D1a1 (Aj271654)
Vesicomya gigas gill symbiont (AF035726)
Thiotrophic bacterial endosymbiont of Bathymodiolus sp. (Aj745718)
Thiotrophic endosymbiont of Bathymodiolus puteoserpentis (Am083975)
Bathymodiolus septemdierum thioautotrophic gill symbiont (Ab036709)
Methylophaga marina (X87338)
Rimicaris exoculata clone SC16S36
Rimicaris exoculata clone LBI32
Hydrothermal Vent Gastropod clone SF_C9-E4 (Ay531557)
carbonate chimney in Lost City clone LCL228B-46 (Dq270625)
Bathymodiolus platifrons methanotrophic gill symbiont (Ab036710)
Methanotrophic bacterial endosymbiont of Bathymodiolus (Aj745717)
Methylobacter sp. BB5.1 (AF016981)
Methylomonas methanica (Af150806)
Methylomicrobium buryaticum (AF096093)
sulfide-microbial incubator clone CH2B4 (Dq228654)
Rimicaris exoculata clone LBI23
Desulfocapsa sulfoexigens (Y13672)
Desulfobacterium corrodens (Ay274450)
Rimicaris exoculata clone SC16S40
carbonate chimney in Lost City clone LCII33B-90 (Dq270648)
Marinosulfonomonas methylotropha clone Se69 (Ay771769)
Rimicaris exoculata clone SCAII26
Methylocapsa acidiphila (Aj278726)
Bacillus subtilis (Ab016721)
Caminicella sporogenes (Aj320233)
Epsilon Proteobacteria
Gamma Proteobacteria
Thiotrophic symbionts
Methanotrophic symbionts
Delta proteobacteria
Alpha Proteobacteria
0.023

Figure 8

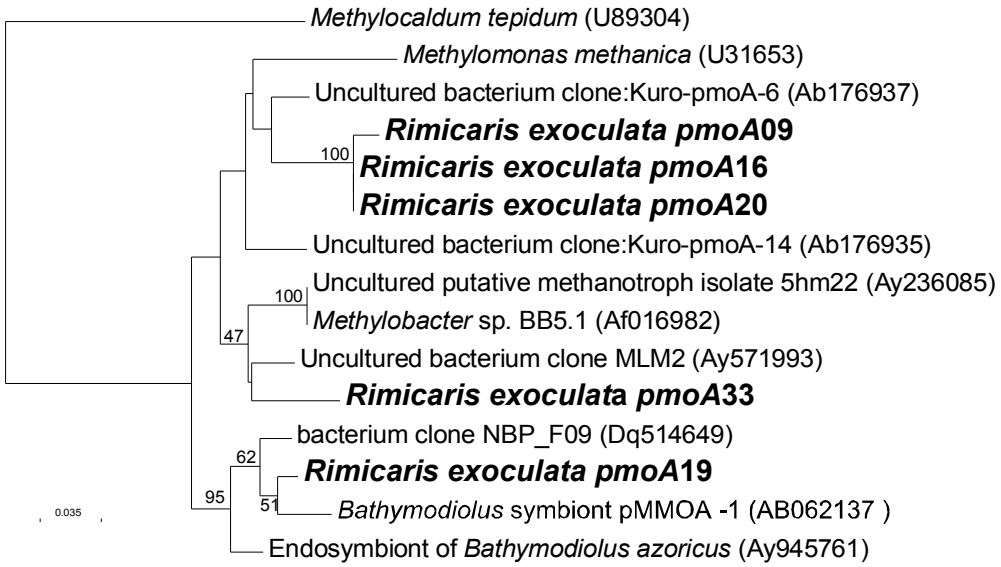
Methylocaldum tepidum (U89304)
Methylomonas methanica (U31653)
Uncultured bacterium clone:Kuro-pmoA-6 (Ab176937)
***Rimicaris exoculata pmoA*09**
100
***Rimicaris exoculata pmoA*16**
***Rimicaris exoculata pmoA*20**
Uncultured bacterium clone:Kuro-pmoA-14 (Ab176935)
Uncultured putative methanotroph isolate 5hm22 (Ay236085)
100
Methylobacter sp. BB5.1 (Af016982)
47
Uncultured bacterium clone MLM2 (Ay571993)
***Rimicaris exoculata pmoA*33**
bacterium clone NBP_F09 (Dq514649)
62
***Rimicaris exoculata pmoA*19**
95
51
Bathymodiolus symbiont pMMOA -1 (AB062137)
0.035
Endosymbiont of *Bathymodiolus azoricus* (Ay945761)

Figure 9

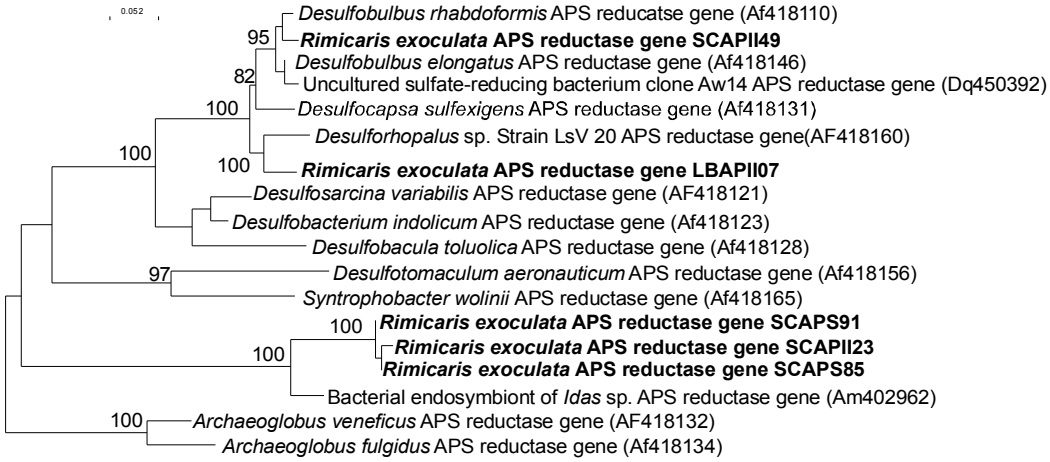
0.052
Desulfobulbus rhabdoformis APS reducatse gene (Af418110)
95
Rimicaris exoculata APS reductase gene SCAPII49
Desulfobulbus elongatus APS reductase gene (Af418146)
82
Uncultured sulfate-reducing bacterium clone Aw14 APS reductase gene (Dq450392)
100
Desulfocapsa sulfexigens APS reductase gene (Af418131)
Desulforhopalus sp. Strain LsV 20 APS reductase gene(AF418160)
100
100
Rimicaris exoculata APS reductase gene LBAPII07
Desulfosarcina variabilis APS reductase gene (AF418121)
Desulfobacterium indolicum APS reductase gene (Af418123)
Desulfobacula toluolica APS reductase gene (Af418128)
97
Desulfotomaculum aeronauticum APS reductase gene (Af418156)
Syntrophobacter wolinii APS reductase gene (Af418165)
100
Rimicaris exoculata APS reductase gene SCAPS91
100
Rimicaris exoculata APS reductase gene SCAPII23
Rimicaris exoculata APS reductase gene SCAPS85
Bacterial endosymbiont of Idas sp. APS reductase gene (Am402962)
100
Archaeoglobus veneficus APS reductase gene (AF418132)
Archaeoglobus fulgidus APS reductase gene (Af418134)

Table 1 : Cell sizes of the various bacterial morphotype observed (values are given in µm and correspond to the upper values measured).

	Cell diameter	Cell height
Large filament	5,5	2,45
Thin filament (1)	1,1	2,35
Thin filament (2)	1,5	2,75
Thick rods (type 1)	0,6	1,25
Thin rods (type 2)	0,3	3

Table 2 : Total numbers of bacteria analyzed, with number of granules and spots for each treatment.

	Bacterial cells	Granules	Spots
Reference shrimps	1574	721	875
Non-sulfide shrimps	3110	911	219
Sulfide shrimps	1883	628	207